scientific reports

Check for updates

OPEN

Assessing the carbonisation temperatures recorded by ancient charcoals for $\delta^{13}C$-based palaeoclimate reconstruction

C. Mouraux[1], F. Delarue[1]✉, J. Bardin[2], T. T. Nguyen Tu[1], L. Bellot-Gurlet[3], C. Paris[3], S. Coubray[4] & A. Dufraisse[4]

Ancient charcoal fragments, produced by the use of wood as fuel in archaeological contexts or during natural or anthropic forest fires, persist in soil and sediments over centuries to millennia. They thus offer a unique window to reconstruct past climate, especially palaeo-precipitation regimes thanks to their stable carbon isotope composition. However, the initial $\delta^{13}C$ of wood is slightly modified as a function of the carbonisation temperature. Carbonisation-induced ^{13}C fractionation is classically investigated through a transfer function between experimental carbonisation temperatures and the carbon content. This approach assumes that the carbon content is conservative through time in ancient charcoals and neglects the potential impact of post-depositional oxidation occurring in soils and sediments. In the present study, we first show that post-depositional oxidation can lead to a large underestimation of past carbonisation temperatures, thereby minimising the estimation of carbonisation-induced ^{13}C fractionations and possibly biasing $\delta^{13}C$-based climate reconstructions. Secondly, by combining carbon content, Fourier-transform infrared and Raman spectroscopy, we propose a new framework to assess the carbonisation temperatures registered in ancient charcoals. This new framework paves the way to reassessing $\delta^{13}C$-based climate reconstruction.

The stable carbon isotope composition ($\delta^{13}C$) of woods is a function of the $^{13}C/^{12}C$ ratio of the initial wood, which depends on environmental conditions such as hydric stress, temperature, the isotope composition of CO_2 and of the photosynthetic carbon fixation pathway[1–7]. The $\delta^{13}C$ of woods ($\delta^{13}C_{wood}$) is therefore widely used to infer past environmental changes[8–11].

In contrast to wood remnants, charred woods, e.g. charcoals, persist in soils and sediments over centuries and millennia owing to their chemical structure dominated by aromatic units, which limits their biological and abiotic degradation with time[12]. Produced by the use of wood as fuel in archaeological contexts or during natural or anthropic forest fires, charcoals are commonly found in soils and sediments. The $\delta^{13}C$ values of charcoals ($\delta^{13}C_{char}$) have therefore been proposed as a useful proxy to assess changes in past environmental conditions—especially paleo-precipitation regimes—provided carbonisation-induced ^{13}C fractionation is non-significant or is corrected[13–15].

Expressed as $\Delta^{13}C$ ($\Delta^{13}C = \delta^{13}C_{char} - \delta^{13}C_{wood}$), this ^{13}C fractionation depends on the carbonisation temperatures undergone by the woods. ^{13}C fractionation can be explained by the kinetic isotope effect and source-induced isotopic fractionations. In the specific case of wood carbonisation, it has been demonstrated that ^{13}C fractionation was mainly driven by the thermal degradation of isotopically distinct biomolecules presenting distinct thermostabilities[16–18]. Several investigations have demonstrated that $\Delta^{13}C$ modifications are directly related to the ^{13}C isotope composition of thermolabile organic moieties degraded in the course of carbonisation[16–18]. Between ca. 180 °C and ca. 450 °C, the thermal degradation of ^{13}C-enriched hemicelluloses and cellulose and the subsequent relative enrichment in ^{13}C-depleted lignin have been shown to yield a reduction in bulk $\delta^{13}C$ values close to the value determined on lignin[13,16–18]. In oak and pine woods, taxa commonly identified in European archaeological sites, carbonisation can therefore yield $\Delta^{13}C$ reaching − 1.4 (600 °C) and − 2.0 ‰ (800 °C),

[1]CNRS, EPHE, PSL, UMR 7619 METIS, Sorbonne Université, 4 place Jussieu, 75005 Paris Cedex 05, France. [2]CNRS, MNHN, UMR 7207 CR2P, Sorbonne Université, 4 place Jussieu, 75005 Paris, France. [3]CNRS, UMR 8233 MONARIS, Sorbonne Université, 4 place Jussieu, 75005 Paris, France. [4]UMR 7209 – AASPE-CNRS/MNHN, Archéozoologie, Archéobotanique: Sociétés, Pratiques et Environnements, CP56, 55 rue Buffon, 75005 Paris, France. ✉email: frederic.delarue@upmc.fr

respectively[17]. These $\Delta^{13}C$ values are in the range of the $\delta^{13}C$ variations determined in uncharred wood used to reconstruct past climate conditions[19,20]. Hence, $\Delta^{13}C$ should be evaluated before using the $\delta^{13}C$ of charcoals as a proxy to assess paleoclimatic changes.

Depending on the carbonisation temperature recorded by charcoals, $\Delta^{13}C$ corrections are usually performed following a transfer function expressing $\Delta^{13}C$ values as a function of the carbon content (%C) determined in experimentally produced charcoals[13,14,21]. Since carbonisation implies a loss of aliphatic units, oxygenated groups and other chemical groups containing heteroelements[22,23], the chemical structure of the wood becomes progressively enriched in condensed aromatic units implying in turn, a well-known rise in %C with carbonisation temperature. However, using %C to assess carbonisation temperatures in ancient charcoals presupposes that %C is conservative through time. Expressed in mass percentage, %C does not only depend on the carbonisation temperatures undergone by woods but also on the modifications in the concentration of other organic and inorganic elements that can occur during post-depositional processes and related charcoal aging processes[24,25]. Additionally, no significant modification in $\delta^{13}C_{char}$ values determined on charred woods was recorded after short-term burial experiments, suggesting that microbial and abiotic degradation has a negligible effect[26–28]. Hence, $\delta^{13}C_{char}$ variations may strictly depend on carbonisation in contrast to %C.

Within soils and sediments, it is well known that the initial physicochemical properties (surface morphology, elemental composition, aromaticity, specific surface area, ion exchange capacity) are modified as a consequence of seasonal climate events (freeze–thaw and wetting–drying cycles), photochemical degradation, biodegradation and oxidation[29,30]. The oxidation of charcoals involves the formation of carboxylic and phenolic groups which in turn, implies a rise in %O compared to %C[24,29,31,32]. Hence, a subtle rise in the O content can induce a lowering of the %C. As cascade consequences, post-depositional oxidation may therefore underestimate carbonisation temperatures and $\Delta^{13}C$ values, biasing in turn paleoclimatic reconstruction.

The Raman "thermometer" seems a promising tool to assess the carbonisation temperatures undergone by charred woods[33,34]. Raman spectroscopy has been demonstrated to be efficient in determining carbonisation temperatures in the 500–1000 °C range[33,34]. However, this Raman "thermometer" cannot estimate carbonisation temperatures between 350 and 450 °C, a range that has often been estimated in many ancient charcoals[13,14,21]. It has indeed been claimed that "*the usual range of carbonization temperatures appears to be relatively restricted in the fossil record*"[13] (around 350–450 °C). This assertion seems, however, at odds with the 600–1000 °C temperature range undergone by wood in open fire[23,24]. This discrepancy suggests that a new methodological framework—independent of post-depositional processes—is necessary to (i) assess the carbonisation temperatures to which ancient charcoals were subjected and (ii) further optimise the use of $\delta^{13}C_{char}$ as a palaeoenvironmental proxy.

The aims of this study were therefore (i) to illustrate the effect of oxidation on %C through a literature survey and (ii) to propose a framework to evaluate the carbonisation temperatures undergone by charcoals and $\Delta^{13}C$ modifications. To this end, we investigated the %C, the ^{13}C isotope composition and the chemical structure of charred *Quercus petraea* and *Pinus sylvestris* woods produced experimentally. The chemical structure of the charcoals was assessed by Fourier Transform infrared (FTIR) and Raman spectroscopies.

Results and discussion

Illustrating the potential effect of post-depositional oxidation on the determination of carbonisation temperatures by %C. Determined in fresh charcoals from *Q. petraea* and *P. sylvestris*, %C varies from 49.6 ± 0.8 (standard deviation) to 86.3 ± 3.1% and from 48.4 ± 0.8 to 90.6 ± 1.8%, respectively. %C is tightly related to pyrolysis temperatures, especially between 300 and 600 °C in accordance with a previous investigation[13] (Fig. 1). Beyond 600 °C, %C remains roughly stable and does not allow any distinction between pyrolysis temperatures. The %C-based thermometer is therefore not suited to assess the carbonisation temperatures ranging between 600 and 1000 °C often measured in archaeological contexts[23,24].

In addition to this first drawback, the use of %C to assess carbonisation temperatures may be biased by oxidation and the related increase in %O[29,30]. This was confirmed by a compilation of data from the literature (Fig. S1) evidencing the expected negative relationship between %C and %O in fresh charcoals resulting from the simultaneous rise in aromaticity and carbonisation temperature. As for fresh charcoals, aged charcoals also tend to present a negative relationship between %C and %O (Fig. S1). However, In contrast to fresh charcoals, aged charcoals are often characterised by higher and lower contributions of O and C, respectively, as a consequence of oxidation (Fig. S1). By comparing charcoals from an active and from pre-industrial kilns situated in Belgium, Hardy et al.[35] suggested that a 200-year post-depositional history can yield (i) an increase in %O ranging between 10.3 and 13% and (ii) a decrease in %C ranging between 27 and 29%. Comparison between fresh and Terra Preta charcoals suggests that oxidation can also strongly modify the O/C atomic ratio from ca. 0.1 to 0.6[29]. For example, applying such an oxidation to a fresh charcoal formed at 700 °C for which a %C and %O of ca. 85% and 10%, respectively should be determined (Fig. 1; Fig. S1), a theoretical %O of ca. 0.4% and a maximum %C of 56% were determined. We use the term "maximum" as, in the proposed calculation, the masses of C (85%) and of other elements (5%), except O, are considered unmodified. Following the relationship between %C and carbonisation temperatures (Fig. 1), this extreme oxidation would imply a carbonisation temperature of ca. 415 ± 32 °C although fresh charcoal was formed at 700 °C. These examples illustrate how the use of %C as a "paleothermometer" for ancient charcoals can substantially underestimate the carbonisation temperatures as a consequence of charcoal oxidation through time. However, it does not mean that oxidation systematically induces this bias but rather that additional tools are required to reconstruct past carbonisation temperatures. In the following, we will therefore discuss the contribution of FTIR and Raman spectroscopy to evaluate carbonisation temperatures in ancient charcoals.

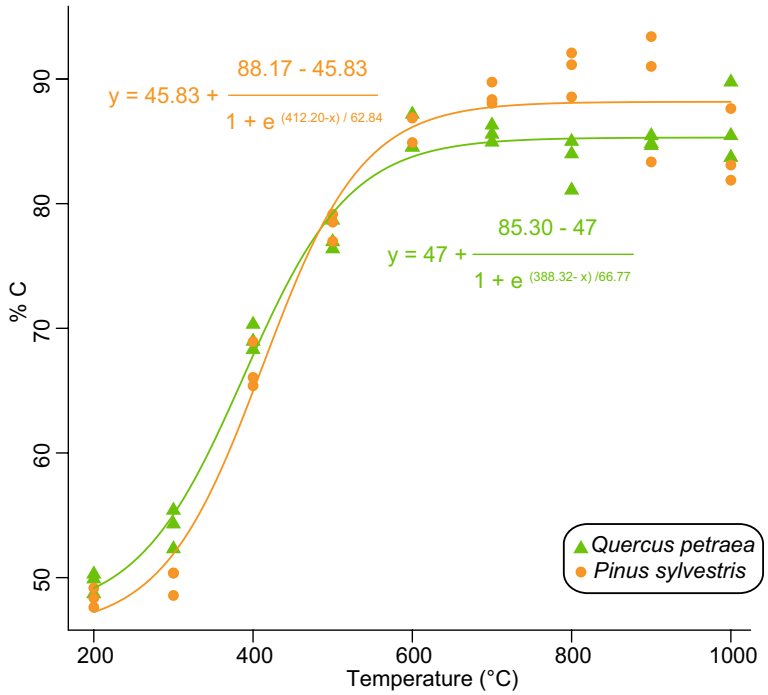

Figure 1. Relationships between carbonisation temperatures and %C in oak and pine charred woods.

FTIR spectroscopy as a tool to evaluate low carbonisation temperatures. In both charred woods from *Q. petraea* and *P. sylvestris*, an increasing pyrolysis temperature implies a reduction in all FTIR peak intensities (e.g. –OH, C=O, C–O–C, C-O, CH_X) compared to the 1600 cm^{-1} band assigned to C=C in aromatics (Table S1; Fig. S2). As expected, most changes in the chemical structure of charred wood occurred between 300 and 400 °C (Fig. S2). Above 400 °C, FTIR spectra were dominated by the C=C intensity peak and no further structural modifications were recorded, suggesting that most of the thermolabile compounds—including cellulose and hemicelluloses—were thermally degraded (Fig. S2). These results are in line with previous investigations evidencing that pyrolysis between 300 and 500 °C entails the thermal decomposition of cellulose and hemicelluloses[36,37]. Among the observed FTIR peaks, those in the 3600–3000 cm^{-1} and in the 1015–1060 cm^{-1} regions can be of interest as they are usually assigned to O–H stretching and to a combination of C–O stretching and O–H deformation related to cellulose and hemicellulose, respectively (Table S1). As the FTIR absorption band in the 3600–3000 cm^{-1} region can be affected by O–H from water[38], the thermal degradation of cellulose and hemicelluloses with carbonisation was therefore tracked here using the $I_{1015\text{-}1060}/I_{1600}$ ratio. Between 300 and 400 °C, the $I_{1015\text{-}1060}/I_{1600}$ ratio dramatically decreased from 4.9 ± 0.2 to 0.2 ± 0.02 and from 8.1 ± 0.3 to 0.3 ± 0.1 in *Q. petraea* and *P. sylvestris,* respectively, as a consequence of cellulose and hemicellulose thermal degradation (Fig. 2). Following this, a relationship between carbonisation temperatures and the $I_{1015–1060}/I_{1600}$ was observed (Fig. 2):

$$I_{1015-1060}/I_{1600} = 5.05 + \frac{0.19 - 5.05}{1 + e^{(304.26 - T°C)/27.88}} \text{ for charred oak} \quad (1)$$

$$I_{1015-1060}/I_{1600} = 8.14 + \frac{0.37 - 8.14}{1 + e^{(327.01 - T°C)/27.43}} \text{ for charred pine} \quad (2)$$

Most of the fossil charcoal record is thought to have been produced at low carbonisation temperatures ranging between 350 °C and 450°C[13,14,21]. If these estimated carbonisation temperatures are correct, a significant content of cellulose and hemicellulose should still be preserved in these ancient charcoals provided that the remnants of cellulose and hemicellulose were not degraded during post-depositional processes. As charcoals are increasingly enriched in condensed aromatic rings during carbonisation, they have long been thought to be insensitive or weakly sensitive to biodegradation because of their carbon structure and possibly, the presence of carbonisation by-products that inhibit enzymatic activities[39]. However, there is compelling evidence for a significant biodegradation of charcoal with time and therefore, a modification of its initial geochemical signatures[40,41]. As charcoals are often considered as being composed of a highly condensed carbon structure, most investigations into biodegradation have focused on the oxidation of the aromatic structure. However, our results and previous investigations demonstrated that significant amounts of polysaccharides can be preserved within charcoals especially those formed at low carbonisation temperature[42–44]. This suggests that a readily available substrate

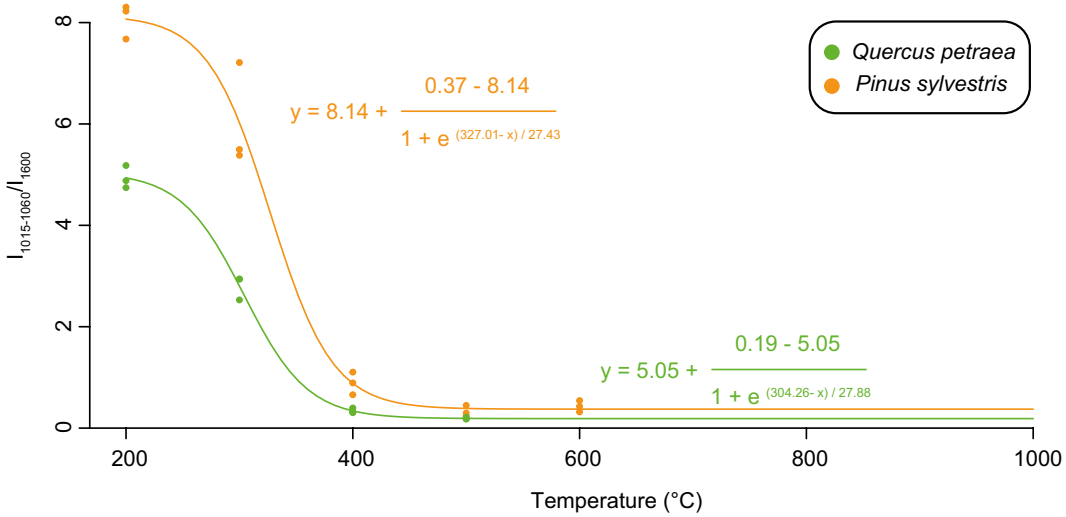

Figure 2. Relationships between the $I_{1015–1060}/I_{1600}$ and carbonisation temperatures in oak and pine charred woods.

may be still available for microbial activities. To date, the biodegradation of remnants of hemicellulose/cellulose within charcoal remains undocumented. Considering this gap in extant knowledge but also the overlapping of FTIR bands due to the occurrence of the inorganic fraction[45], we suggest that the application of the FTIR thermometer should be restricted to fresh charcoals devoid of ash. Nonetheless, the occurrence of FTIR bands typically related to the preservation of cellulose/hemicellulose is an essential observation for diagnosing a carbonisation temperature below 400 °C in ancient charcoals. In other words, and after a careful rinsing to avoid carbohydrates originating from biofilms, such FTIR bands should be observed in most of the fossil charcoal record which was proposed to have been produced at ca. 400 °C—if preserved against soil/sediment microbial decomposition activities[13,14,21].

Raman thermometry. In contrast to archaeological charcoals putatively produced at low carbonisation temperatures, several investigations suggested that some archaeological charcoals underwent a carbonisation temperature ranging between 600 and 1000 °C (house fires, pottery kilns, etc.). In this temperature range, Raman spectroscopy has been demonstrated to be efficient in determining the carbonisation temperature[23,33,34]. These pioneering works suggested that Raman-derived parameters can assess the carbonisation temperature—ranging between 500 and 1200 °C—undergone by both charred pine and oak woods. In this study, the fluorescence level was too high to record any Raman spectra in *Q. petraea* and in *P. sylvestris*, respectively, below 400 °C and 500 °C. This may be a consequence of the aliphatic content remaining in charred wood at such carbonisation temperatures as suggested by FTIR spectra (see the occurrence of CH_2 bonds in the 2850–2920 cm^{-1} FTIR band region; Fig. S2). At and beyond these carbonisation temperatures, we observed the well-known "carbonisation trend" determined in a wide range of carbonaceous materials subjected to thermal degradation[23,46,47] (Fig. S3). This carbonisation trend consists in a simultaneous rise (i) in the A_D/A_G ratio from 1.15 to 1.82 and from 1.22 to 1.77 and (ii) in the H_D/H_G ratio from 0.55 to 0.93 and from 0.58 to 0.93 in both *Q. petraea* and in *P. sylvestris* charred woods, respectively (Fig. 3).

A_D/A_G and H_D/H_G ratios can both be used to assess carbonisation temperatures between 400 and 1000 °C in the studied charred woods.

$$\mathrm{AD/AG} = 1.04 + \frac{1.77 - 1.04}{1 + e^{(607.96 - T°\mathrm{C})/97.11}} \text{ for charred oak} \quad (3)$$

$$\mathrm{AD/AG} = 1.01 + \frac{1.88 - 1.01}{1 + e^{(622.55 - T°\mathrm{C})/135.76}} \text{ for charred pine} \quad (4)$$

$$\mathrm{HD/HG} = 0.56 + \frac{0.93 - 0.56}{1 + e^{(715.49 - T°\mathrm{C})/82.25}} \text{ for charred oak} \quad (5)$$

$$\mathrm{HD/HG} = 0.55 + \frac{0.95 - 0.55}{1 + e^{(732.09 - T°\mathrm{C})/99.16}} \text{ for charred pine} \quad (6)$$

Based on the integration of the complex and broad D band, the A_D/A_G ratio is highly sensitive to the modification in the shape of D sub-bands. Occurring at ca. 1350 cm^{-1}, the D1-band is related to heteroatoms, vacancies and structural defects[23,48] (Fig. S3). During carbonisation, the D1 band intensity therefore irreversibly increases as a consequence of the resulting increase in the size of the polyaromatic layers[34]. Moreover, the D5 sub-band, which

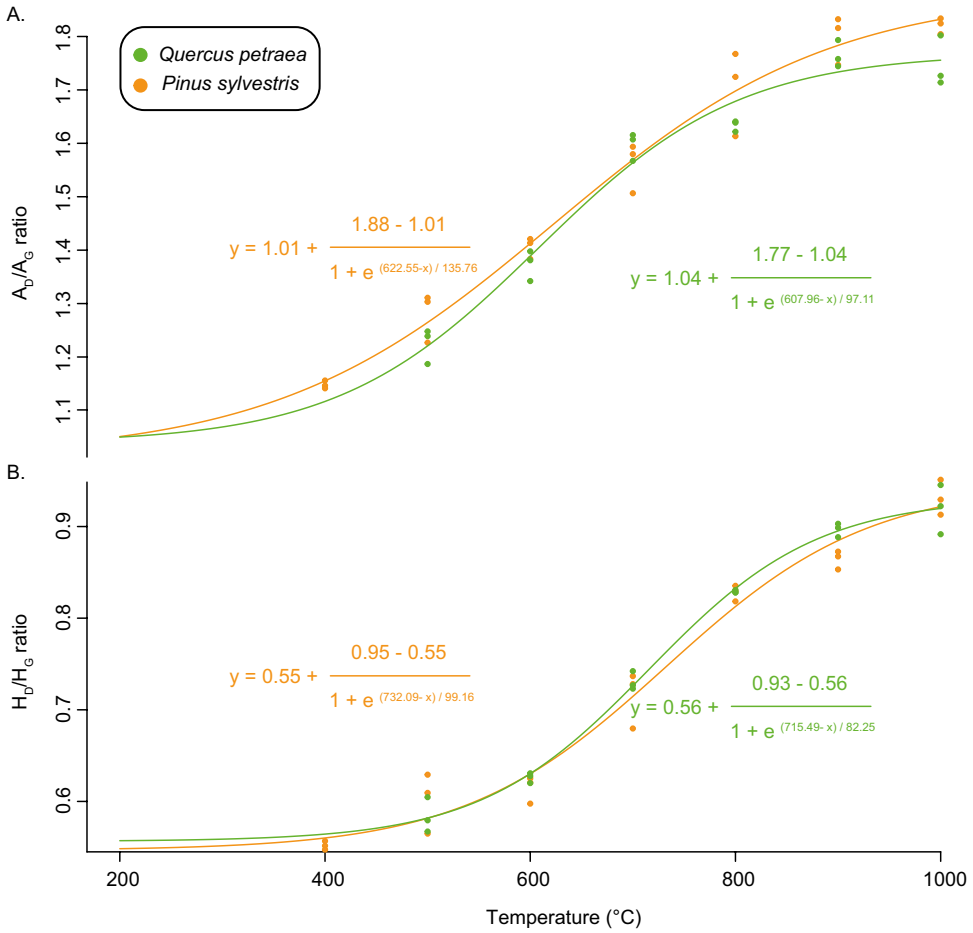

Figure 3. Relationships between (**A**) the A_D/A_G and (**B**) H_D/H_G ratios and carbonisation temperatures in oak and pine charred woods.

occurs at ca. 1450 cm^{-1} (Fig. S3), is thought to diagnose the presence of aliphatic hydrocarbons (i) entrapped within the nanoporosity of the macromolecular network and (ii) degraded in the course of carbonisation[23,49].

Reconsidering the determination of past carbonisation temperatures to correct $\delta^{13}C$ in ancient charcoals.. A decrease in $\delta^{13}C_{char}$ values during charring is a well-known process[16–18]. Most of the carbonisation-induced $\delta^{13}C$ modifications take place below a temperature of 400 °C (Fig. 4), a temperature at which most of the cellulose and hemicellulose—relatively enriched in ^{13}C—is thermally degraded[13,16–18]. From 200 to 600 °C, $\delta^{13}C_{char}$ values decrease from −28.1 ± 0.04 to -29.8 ± 0.1‰ and from −25.5 ± 0.1 to −27.6 ± 0.04 ‰ in charred oak and pine woods, respectively (Fig. 4). Between 600 and 1000 °C, no clear modifications of the $\delta^{13}C$ values were observable (Fig. 4). In this latter temperature range, $\delta^{13}C_{char}$ exhibits values from −29.9 ± 0.2 to −29.7 ± 0.3 ‰ and from −27.4 ± 0.2 to −27.6 ± 0.1 ‰ in charred oak and pine woods, respectively (Fig. 4). Our results suggest that a maximum $\Delta^{13}C$ value of 1.8 and 2.2‰ is reached for charred oak and pine woods, respectively (Fig. 4).

Classically, the effect of carbonisation is corrected following a transfer function using %C to assess carbonisation temperatures[13,14,21]. However, as stressed before, %C can be potentially biased by the oxidation occurring during post-depositional processes but also be limiting to assess carbonisation temperatures above 600 °C. Since the application of the FTIR thermometer is restricted to fresh charcoal, only Raman-derived parameters seem appropriate to determine carbonisation temperatures (as the studied Raman parameters seem to be insignificantly modified by post-depositional processes[50]). However, as the typical D and G bands arise after 400 °C—the temperature at which most of the carbonisation-induced ^{13}C fractionation occurs—Raman thermometers cannot be used to propose a transfer function between $\delta^{13}C_{char}$ and carbonisation temperature or $\delta^{13}C_{wood}$. Nonetheless, the combination of %C, FTIR and Raman spectroscopies can provide a framework to assess and/or reassess the carbonisation temperatures undergone by charred oak and pine woods following the scheme provided in Fig. S4.

FTIR spectroscopy is the first step in this framework. After a thorough preliminary treatment to avoid the occurrence of exogenous OM, the observation of the FTIR band at ca. 1045 cm^{-1}—related to C-O bonds in hemicellulose and cellulose—shows that carbonisation temperatures were below 400 °C. Nonetheless, one should keep in mind that a subtle modification in the %O can lead to a large underestimation of carbonisation temperatures

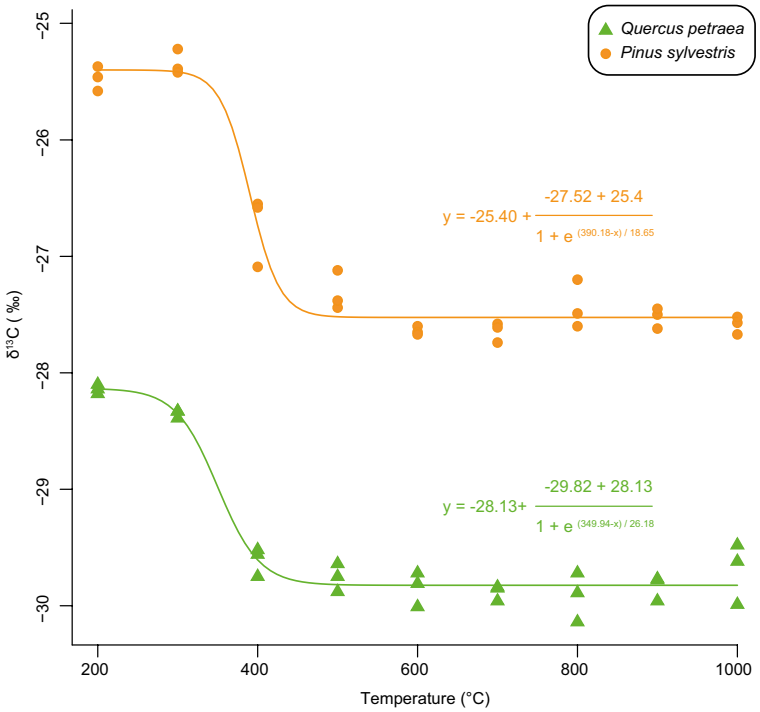

Figure 4. Modifications of $\delta^{13}C_{char}$ values with carbonisation temperatures in charred oak and pine charred woods.

in particular in the 300–400 °C range where %C and $\delta^{13}C$ are strongly modified. In addition, it is worth noting that carbonisation below 400 °C cannot be ruled out in the absence of both hemicellulose/cellulose FTIR bands because of microbial decomposition occurring during post-depositional processes. In this respect, the absence of Raman spectra (below 400 and 500 °C for oak and pine charred woods) is a key observation and should have profound implications for reassessing the carbonisation temperatures of ancient charcoals used for palaeoclimate reconstruction. If most charcoals in the fossil record were indeed produced below a temperature of ca. 400 °C, they should lack the D and G bands observed with Raman spectroscopy. If this condition is not fulfilled, it would suggest that $\Delta^{13}C$ may be underestimated by up to 1‰, a value in the range of the climate-induced $\delta^{13}C$ variations determined in uncharred wood[19,20]. Above 600 °C, ^{13}C modifications reach a maximum value, implying a direct correction of carbonisation-induced ^{13}C fractionation through a simple subtraction. This is the only case for which a univocal correction of $\delta^{13}C$ values is possible (Fig. S4). Hence, in archaeological settings where charcoals were formed in a variety of contexts (on open fires, house burning, kilns, etc.) and registered carbonisation temperatures between 600 and 1000 °C, $\delta^{13}C_{char}$ can be directly compared to assess palaeo-precipitation regimes provided they were measured on a single tree species. A simple subtraction of $\delta^{13}C_{char}$ by the maximum $\Delta^{13}C$ value can also be considered to assess $\delta^{13}C_{wood}$ according to $\delta^{13}C_{char}$.

In the case of charcoals that experienced carbonisation temperatures below 600 °C, such a scheme cannot be directly applied. We therefore propose that these charred woods should be recarbonised until reaching the carbon structural order observed here at a temperature of 600 °C. By taking advantage of the irreversibility of chemical changes occurring during carbonisation, this recarbonisation step implies that the maximum $\Delta^{13}C$ value will be theoretically reached. In addition to allowing a direct comparison between $\delta^{13}C_{char}$ determined in charcoals from a single species, the main advantage of this simplistic approach is that it (i) avoids all uncertainties related to oxidation and the use of the %C "thermometer" and (ii) minimises error propagation related to the determination of $\Delta^{13}C$ values in the course of carbonisation.

Conclusion

Determining the evolution of past climate is of fundamental interest to understand interactions between past societies and climate change. To this end, charcoal macro-remains, which are the most frequent modes of wood conservation in archaeological sites, thus represent a key record. Their ^{13}C isotope composition can yield valuable information provided the effects of carbonisation and of post-depositional oxidation are constrained. Here we show that post-depositional oxidation—a subsequent rise in %O—can bias the determination of carbonisation temperatures through %C. By reducing the %C, post-depositional processes can therefore lead to an underestimation of carbonisation temperatures implying in turn, an inappropriate correction of carbonisation-induced ^{13}C fractionation. By studying the chemical structure of *Q. petraea* and *P. sylvestris* charred woods formed between 200 and 1000 °C in an inert atmosphere, our results tend to question previous evidence for carbonisation temperatures below 400 °C in some archaeological charcoals. Two main criteria were identified to ensure that these archaeological charcoals were indeed formed below 400 °C:

- Preservation of cellulose and hemicellulose observed through infrared spectroscopy provided they were preserved against biodegradation;
- Lack of the typical Raman D and G bands classically observed in Raman spectroscopy.

Above an apparent carbonisation temperature of 600 °C, $\Delta^{13}C$ remains stable, suggesting that no ^{13}C corrections or a direct correction of carbonisation through the simple subtraction of $\delta^{13}C_{char}$ by the maximum $\Delta^{13}C$ is required. Following our conclusions, we suggest that a thorough examination of the chemical structure of ancient charcoals is required to assess and reassess past climate changes using the ^{13}C isotope composition.

Methods

Experimental carbonisation. Charcoal samples were produced experimentally in the laboratory from crushed oak (*Q. petraea*) and pine (*P. sylvestris*) woods. Powdered wood was chosen to limit any physical roughness and chemical heterogeneity that might induce a change in the mean response to carbonisation. *Q. petraea* and *P. sylvestris* were subjected to pyrolysis in a furnace pyrolyser under N_2 flow (O_2-free atmosphere). The samples (ca. 200 mg) were placed in a quartz tube plugged with quartz wool that was then heated for 1 h at 200, 300, 400, 500, 600, 700, 800, 900 and 1000 °C. It is worth mentioning that heating durations varied between 20 min to 15 h in previous carbonisation experiments[16,17,51,52]. A previous investigation demonstrated that a heating duration above 1 h has little effect on the degree of aromaticity of charcoals recorded with Raman spectroscopy[33]. In contrast, there is still no clear evidence that heating durations below 1 h are enough to reach a similar degree of aromaticity. Hence, a heat duration of 1 h was chosen to minimise the effect of heat duration on the selected carbonisation temperatures. All pyrolysis were performed in triplicate.

Carbon concentration and $\delta^{13}C$ values. Approximately 0.2–0.3 mg of charcoal were combusted using an elemental analyser (Thermo Fisher Scientific Flash, 2000) coupled to an isotope ratio mass spectrometer (Thermo Fisher Scientific Delta V advantage) to determine both %C and $\delta^{13}C$. Uncharred oak wood, tyrosine and urea were used as internal standards (standard deviation of ca. 0.1‰). Internal standard true values, measured values and standard deviations are provided in supplementary Table 2.

Fourier transform infrared spectroscopy. FTIR spectroscopy was performed by attenuated total reflectance FTIR spectroscopy using a Bruker Tensor 27 spectrometer. The powdered uncharred and charred materials were placed directly on a germanium crystal. FTIR spectra were acquired by 64 scans at a 2 cm^{-1} resolution over the range 4000–600 cm^{-1}. All spectra were corrected for water vapour, CO_2 and for differences in depth of beam penetration at different wavelengths (ATR correction; Opus software). All spectra were then normalised. For each spectrum, standardisation involved a subtraction of the minimum absorption value applied to the whole spectrum followed by a multiplication—applied on the whole spectrum—to obtain a similar spectral maximum absorbance value for all uncharred and charred woods[53]. The $I_{1015\text{-}1060}/I_{1600}$ intensity ratio was then computed to track the fate of cellulose/hemicelluloses during carbonisation at low pyrolysis temperature. Assignments of FTIR absorption bands are summarised in supplementary Table 1.

Raman spectroscopy. Raman spectroscopy was performed using a MR800 Horiba Jobin Yvon spectrometer equipped with a 514.5 nm green laser. The laser was focused on the sample with a 50 × objective. The spectrometer was first calibrated with a silicon standard before the analytical session (matching at 520.5 cm^{-1}). A laser power below 1 mW was used to prevent any thermal alteration during spectrum acquisition[54,55]. Spectrum acquisition was achieved after three iterations using a time exposure of 180 s (spectral resolution of 2 cm^{-1}). For each sample, we determined the Raman shift intensity in the 600 to 2300 cm^{-1} spectral window including the first-order disorder (D) and graphite (G) peaks centred at about 1350 and 1600 cm^{-1}, respectively. The D band is a complex band assigned to defects in the aromatic structure (e.g. functional groups, heteroatoms and vacancies) and to amorphous carbon tightly associated with the macromolecular network[48,56]. The G band is ascribed to in-plane stretchings of C=C bonds within graphene-like clusters[48]. After linear baseline correction, two Raman-derived parameters were computed: the A_D/A_G and the H_D/H_G ratios. The A_D/A_G ratio is the ratio between the integrated D (between 1000 and 1500 cm^{-1}) and G areas (between 1500 and 1800 cm^{-1}).The H_D/H_G ratio corresponds to the ratio between the maximum peak intensity of the D and G peaks.

Statistics. To evaluate the relationship between carbonisation temperatures and the chemical structure of charcoals, regression models were used. All the variables under study (i.e. the %C, the ^{13}C isotope composition, the $I_{1015\text{-}1060}/I_{1600}$ intensity ratio, the A_D/A_G and the H_D/H_G ratios) vary with the temperature following S-shaped curves. The generalised logistic function (also known as Richard's function) was therefore used to perform regressions.

$$Y(T°C) = a + \frac{b-a}{1+e^{(xm-T°C)/s}} \quad (7)$$

This function depends on five parameters: *a*, the asymptote for low temperatures, is the initial condition before carbonisation; *b*, the asymptote for high temperatures, corresponds to the state of the sample for a theoretical infinite temperature; *xm*, corresponds to the middle of the S-curve, in other words, the temperature where half of the process has been completed; *s* quantifies the curvature of the S-curve. To determine the least-squares estimates of the parameters, we used the *nls* function of the *stats* package[57]. To estimate the error in predicting the responses given a temperature, 95% prediction intervals were computed using the *propagate* package. However,

when one wants to use the regressions done herein to predict a temperature given a response (e.g. obtaining a temperature given an A_D/A_G ratio), the calibration error has to be added. For that purpose, we used the delta method as described in Huet et al.[58] which has the advantage of accounting for both the variability of the response and the uncertainty about the calibration curve.

Based on literature data, a regression between the oxygen content (%O) and %C determined in fresh and aged charcoals was also conducted (Fig. S1). The regression of the %O against %C is linear in the form $y = ax + b$ and was done with the *lm* function.

Data availability

Data are provided in supplementary table 3.

Received: 7 January 2022; Accepted: 1 August 2022
Published online: 29 August 2022

References

1. Farquhar, G., O'Leary, M. & Berry, J. On the relationship between carbon isotope discrimination and the intercellular carbon dioxide concentration in leaves. *Funct. Plant Biol.* **9**, 121 (1982).
2. van Bergen, P. F. & Poole, I. Stable carbon isotopes of wood: a clue to palaeoclimate?. *Palaeogeogr. Palaeoclimatol. Palaeoecol.* **182**, 31–45 (2002).
3. Leavitt, S. W. Prospects for reconstruction of seasonal environment from tree-ring δ13C: baseline findings from the Great Lakes area, USA. *Chem. Geol.* **192**, 47–58 (2002).
4. Briffa, K. R., Osborn, T. J. & Schweingruber, F. H. Large-scale temperature inferences from tree rings: A review. *Glob. Planet. Change* **40**, 11–26 (2004).
5. McCarroll, D. *et al.* Correction of tree ring stable carbon isotope chronologies for changes in the carbon dioxide content of the atmosphere. *Geochim. Cosmochim. Acta* **73**, 1539–1547 (2009).
6. Shu, Y. *et al.* Relative humidity recorded in tree rings: A study along a precipitation gradient in the Olympic Mountains, Washington, USA. *Geochim. Cosmochim. Acta* **69**, 791–799 (2005).
7. McCarroll, D. & Loader, N. J. Stable isotopes in tree rings. *Quatern. Sci. Rev.* **23**, 771–801 (2004).
8. Feng, X. & Epstein, S. Climatic trends from isotopic records of tree rings: The past 100–200 years. *Clim. Change* **33**, 551–562 (1996).
9. Masson-Delmotte, V. *et al.* Changes in European precipitation seasonality and in drought frequencies revealed by a four-century-long tree-ring isotopic record from Brittany, western France. *Clim. Dyn.* **24**, 57–69 (2005).
10. Meko, D. M. *et al.* Medieval drought in the upper Colorado River Basin. *Geophys. Res. Lett.* **34**, L10705 (2007).
11. Kress, A. *et al.* A 350 year drought reconstruction from Alpine tree ring stable isotopes: Isotope drought reconstruction. *Glob. Biogeochem. Cycles* https://doi.org/10.1029/2009GB003613 (2010).
12. Schmidt, M. W. I. *et al.* Persistence of soil organic matter as an ecosystem property. *Nature* **478**, 49–56 (2011).
13. Ferrio, J. P., Alonso, N., López, J. B., Araus, J. L. & Voltas, J. Carbon isotope composition of fossil charcoal reveals aridity changes in the NW Mediterranean Basin. *Glob. Change Biol.* **12**, 1253–1266 (2006).
14. Aguilera, M., Ferrio, J. P., Pérez, G., Araus, J. L. & Voltas, J. Holocene changes in precipitation seasonality in the western Mediterranean Basin: A multi-species approach using $\delta^{13}C$ of archaeobotanical remains. *J. Quatern. Sci.* **27**, 192–202 (2012).
15. Baton, F. *et al.* Tree-ring δ13C of archeological charcoals as indicator of past climatic seasonality. A case study from the Neolithic settlements of Lake Chalain (Jura, France). *Quatern. Int.* **457**, 50–59 (2017).
16. Czimczik, C. I., Preston, C. M., Schmidt, M. W. I., Werner, R. A. & Schulze, E.-D. Effects of charring on mass, organic carbon, and stable carbon isotope composition of wood. *Org. Geochem.* **33**, 1207–1223 (2002).
17. Turney, C. S. M., Wheeler, D. & Chivas, A. R. Carbon isotope fractionation in wood during carbonization. *Geochim. Cosmochim. Acta* **70**, 960–964 (2006).
18. Ascough, P. L., Bird, M. I., Wormald, P., Snape, C. E. & Apperley, D. Influence of production variables and starting material on charcoal stable isotopic and molecular characteristics. *Geochim. Cosmochim. Acta* **72**, 6090–6102 (2008).
19. Porter, T. J., Pisaric, M. F. J., Kokelj, S. V. & Edwards, T. W. D. Climatic signals in $\delta^{13}C$ and $\delta^{18}O$ of tree-rings from white spruce in the Mackenzie Delta Region, Northern Canada. *Arct. Antarct. Alp. Res.* **41**, 497–505 (2009).
20. Young, G. H. F. *et al.* Central England temperature since AD 1850: the potential of stable carbon isotopes in British oak trees to reconstruct past summer temperatures. *J. Quatern. Sci.* **27**, 606–614 (2012).
21. Audiard, B. *et al.* $\delta^{13}C$ referential in three Pinus species for a first archaeological application to Paleolithic contexts: "Between intra- and inter-individual variation and carbonization effect". *J. Archaeol. Sci. Rep.* **20**, 775–783 (2018).
22. Oberlin, A. Carbonization and graphitization. *Carbon* **22**, 521–541 (1984).
23. Rouzaud, J.-N., Deldicque, D., Charon, É. & Pageot, J. Carbons at the heart of questions on energy and environment: A nanostructural approach. *C.R. Geosci.* **347**, 124–133 (2015).
24. Cohen-Ofri, I., Weiner, L., Boaretto, E., Mintz, G. & Weiner, S. Modern and fossil charcoal: Aspects of structure and diagenesis. *J. Archaeol. Sci.* **33**, 428–439 (2006).
25. Ascough, P. L., Bird, M. I., Francis, S. M. & Lebl, T. Alkali extraction of archaeological and geological charcoal: Evidence for diagenetic degradation and formation of humic acids. *J. Archaeol. Sci.* **38**, 69–78 (2011).
26. DeNiro, M. J. & Hastorf, C. A. Alteration of and ratios of plant matter during the initial stages of diagenesis: Studies utilizing archaeological specimens from Peru. *Geochim. Cosmochim. Acta* **49**, 97–115 (1985).
27. Fraser, R. A. *et al.* Assessing natural variation and the effects of charring, burial and pre-treatment on the stable carbon and nitrogen isotope values of archaeobotanical cereals and pulses. *J. Archaeol. Sci.* **40**, 4754–4766 (2013).
28. Styring, A. K. *et al.* The effect of charring and burial on the biochemical composition of cereal grains: Investigating the integrity of archaeological plant material. *J. Archaeol. Sci.* **40**, 4767–4779 (2013).
29. Wiedner, K. *et al.* Acceleration of biochar surface oxidation during composting?. *J. Agric. Food Chem.* **63**, 3830–3837 (2015).
30. Wang, L. *et al.* Biochar aging: Mechanisms, physicochemical changes, assessment, and implications for field applications. *Environ. Sci. Technol.* **54**, 14797–14814 (2020).
31. Cheng, C.-H., Lehmann, J., Thies, J. E., Burton, S. D. & Engelhard, M. H. Oxidation of black carbon by biotic and abiotic processes. *Org. Geochem.* **37**, 1477–1488 (2006).
32. Heitkötter, J. & Marschner, B. Interactive effects of biochar ageing in soils related to feedstock, pyrolysis temperature, and historic charcoal production. *Geoderma* **245–246**, 56–64 (2015).
33. Deldicque, D., Rouzaud, J.-N. & Velde, B. A Raman–HRTEM study of the carbonization of wood: A new Raman-based paleothermometer dedicated to archaeometry. *Carbon* **102**, 319–329 (2016).
34. Deldicque, D. & Rouzaud, J.-N. Temperatures reached by the roof structure of Notre-Dame de Paris in the fire of April 15th 2019 determined by Raman paleothermometry. *Comptes Rendus Géosci.* **352**, 7–18 (2020).

35. Hardy, B. *et al.* Long term change in chemical properties of preindustrial charcoal particles aged in forest and agricultural temperate soil. *Org. Geochem.* **107**, 33–45 (2017).
36. Murwanashyaka, J. N., Pakdel, H. & Roy, C. Step-wise and one-step vacuum pyrolysis of birch-derived biomass to monitor the evolution of phenols. *J. Anal. Appl. Pyrol.* **60**, 219–231 (2001).
37. Xin, S. *et al.* Chemical structure evolution of char during the pyrolysis of cellulose. *J. Anal. Appl. Pyrol.* **116**, 263–271 (2015).
38. Georgakopoulos, A. Study of low rank greek coals using FTIR spectroscopy. *Energy Sources* **25**, 995–1005 (2003).
39. Weiland, J. J. & Guyonnet, R. Study of chemical modifications and fungi degradation of thermally modified wood using DRIFT spectroscopy. *Holz Roh Werkst* **61**, 216–220 (2003).
40. Ascough, P. L., Sturrock, C. J. & Bird, M. I. Investigation of growth responses in saprophytic fungi to charred biomass. *Isot. Environ. Health Stud.* **46**, 64–77 (2010).
41. Kymäläinen, M., Havimo, M., Keriö, S., Kemell, M. & Solio, J. Biological degradation of torrefied wood and charcoal. *Biomass Bioenergy* **71**, 170–177 (2014).
42. Pastorova, I., Arisz, P. W. & Boon, J. J. Preservation of D-glucose-oligosaccharides in cellulose chars. *Carbohydr. Res.* **248**, 151–165 (1993).
43. Boon, J. J., Pastorova, I., Botto, R. E. & Arisz, P. W. Structural studies on cellulose pyrolysis and cellulose chars by PYMS, PYGCMS, FTIR, NMR and by wet chemical techniques. *Biomass Bioenergy* **7**, 25–32 (1994).
44. Kuzyakov, Y., Bogomolova, I. & Glaser, B. Biochar stability in soil: Decomposition during eight years and transformation as assessed by compound-specific 14C analysis. *Soil Biol. Biochem.* **70**, 229–236 (2014).
45. Pizzo, B., Pecoraro, E., Alves, A., Macchioni, N. & Rodrigues, J. C. Quantitative evaluation by attenuated total reflectance infrared (ATR-FTIR) spectroscopy of the chemical composition of decayed wood preserved in waterlogged conditions. *Talanta* **131**, 14–20 (2015).
46. Bonal, L., Bourot-Denise, M., Quirico, E., Montagnac, G. & Lewin, E. Organic matter and metamorphic history of CO chondrites. *Geochim. Cosmochim. Acta* **71**, 1605–1623 (2007).
47. Delarue, F. *et al.* The Raman-derived carbonization continuum: A tool to select the best preserved molecular structures in Archean Kerogens. *Astrobiology* **16**, 407–417 (2016).
48. Ferralis, N., Matys, E. D., Knoll, A. H., Hallmann, C. & Summons, R. E. Rapid, direct and non-destructive assessment of fossil organic matter via microRaman spectroscopy. *Carbon* **108**, 440–449 (2016).
49. Romero-Sarmiento, M.-F. *et al.* Evolution of Barnett Shale organic carbon structure and nanostructure with increasing maturation. *Org. Geochem.* **71**, 7–16 (2014).
50. Inoue, J., Yoshie, A., Tanaka, T., Onji, T. & Inoue, Y. Disappearance and alteration process of charcoal fragments in cumulative soils studied using Raman spectroscopy. *Geoderma* **285**, 164–172 (2017).
51. Jones, T. P. & Chaloner, W. G. Fossil charcoal, its recognition and palaeoatmospheric significance. *Glob. Planet. Change* **5**, 39–50 (1991).
52. Poole, I., Braadbaart, F., Boon, J. J. & van Bergen, P. F. Stable carbon isotope changes during artificial charring of propagules. *Org. Geochem.* **33**, 1675–1681 (2002).
53. Delarue, F. *et al.* Can Rock-Eval pyrolysis assess the biogeochemical composition of organic matter during peatification?. *Org. Geochem.* **61**, 66–72 (2013).
54. Everall, N. J., Lumsdon, J. & Christopher, D. J. The effect of laser-induced heating upon the vibrational Raman spectra of graphites and carbon fibres. *Carbon* **29**, 133–137 (1991).
55. Henry, D. G., Jarvis, I., Gillmore, G. & Stephenson, M. Raman spectroscopy as a tool to determine the thermal maturity of organic matter: Application to sedimentary, metamorphic and structural geology. *Earth Sci. Rev.* **198**, 102936 (2019).
56. Ferrari, A. C. & Robertson, J. Interpretation of Raman spectra of disordered and amorphous carbon. *Phys. Rev. B* **61**, 14095–14107 (2000).
57. R Core Team. *R: A Language and Environment for Statistical Computing* (R Foundation for Statistical Computing, 2018).
58. Huet, S., Bouvier, A., Gruet, M.-A. & Jolivet, E. *Statistical Tools for Nonlinear Regression* (Springer, 1996). https://doi.org/10.1007/978-1-4757-2523-0.41.

Acknowledgements

This work was supported by the Paris Ile-de-France Region through the Domaine d'intéret majeur (DIM) programme: 'Matériaux anciens et patrimoniaux'. This investigation was also supported by Action transverse MITI: Chantier scientifique Notre-Dame de Paris. This work also benefits from the financial support of the « ANR-Agence Nationale de la Recherche" (CASIMODO project; ANR-20-CE03-0008). We are grateful to Mercedes Mendez-Millan (Alysés platform, IRD) for mass spectrometry analyses. We also acknowledge Elizabeth Rowley-Jolivet for English language editing.

Author contributions

C.M.: Investigation, writing of the original draft, review and editing. F.D: Funding acquisition, project administration, conceptualisation, supervision, validation, writing of the original Draft, review and editing. J.B.: Formal analysis, writing of the original draft, review and editing. S.C.: Writing of the original draft, review and editing. T.T.N.T.: Writing of the original draft, review and editing. L.B.-G.: Investigation. C.P.: Investigation. A.D.: Funding acquisition, project administration, conceptualisation, supervision, validation, writing of the original Draft, review and editing.

Competing interests

The authors declare no competing interests.

Additional information

Supplementary Information The online version contains supplementary material available at https://doi.org/10.1038/s41598-022-17836-2.

Correspondence and requests for materials should be addressed to F.D.

Reprints and permissions information is available at www.nature.com/reprints.

Publisher's note Springer Nature remains neutral with regard to jurisdictional claims in published maps and institutional affiliations.

Open Access This article is licensed under a Creative Commons Attribution 4.0 International License, which permits use, sharing, adaptation, distribution and reproduction in any medium or format, as long as you give appropriate credit to the original author(s) and the source, provide a link to the Creative Commons licence, and indicate if changes were made. The images or other third party material in this article are included in the article's Creative Commons licence, unless indicated otherwise in a credit line to the material. If material is not included in the article's Creative Commons licence and your intended use is not permitted by statutory regulation or exceeds the permitted use, you will need to obtain permission directly from the copyright holder. To view a copy of this licence, visit http://creativecommons.org/licenses/by/4.0/.

© The Author(s) 2022